



HAL
open science

Impact of GaN Cap Layer and Carbon-Doped Buffer Layer on Thermal Resistance of HEMTs GaN

Khalil Karrame, Sujan Sarkar, Khade Ramdas Pandurang, Jean-Christophe Nallatamby, Amitava Dasgupta, Nandita Dasgupta, Maggy Colas, Raphaël Sommet

► **To cite this version:**

Khalil Karrame, Sujan Sarkar, Khade Ramdas Pandurang, Jean-Christophe Nallatamby, Amitava Dasgupta, et al.. Impact of GaN Cap Layer and Carbon-Doped Buffer Layer on Thermal Resistance of HEMTs GaN. 2024 30th International Workshop on Thermal Investigations of ICs and Systems (THERMINIC), Sep 2024, Toulouse, France. pp.1-4, 10.1109/THERMINIC62015.2024.10732655 . hal-04774322

HAL Id: hal-04774322

<https://hal.science/hal-04774322v1>

Submitted on 8 Nov 2024

HAL is a multi-disciplinary open access archive for the deposit and dissemination of scientific research documents, whether they are published or not. The documents may come from teaching and research institutions in France or abroad, or from public or private research centers.

L'archive ouverte pluridisciplinaire **HAL**, est destinée au dépôt et à la diffusion de documents scientifiques de niveau recherche, publiés ou non, émanant des établissements d'enseignement et de recherche français ou étrangers, des laboratoires publics ou privés.

Impact of GaN Cap Layer and Carbon-Doped Buffer Layer on Thermal Resistance of HEMTs GaN

Khalil Karrame
Xlim laboratory
7 rue Jules Vallès
19100 Brive-La-Gaillarde, FRANCE
khalil.karrame@xlim.fr

Sujan Sarkar
Indian Institute of Technology Madras,
Chennai-600036, India
ee17d004@smail.iitm.ac.in

Khade Ramdas Pandurang
Indian Institute of Technology Madras,
Chennai-600036, India
ee17d411@smail.iitm.ac.in

Jean-Christophe Nallatamby
Xlim laboratory
7 rue Jules Vallès
19100 Brive-La-Gaillarde, FRANCE
jean-christophe.nallatamby@xlim.fr

Amitava Dasgupta
Indian Institute of Technology Madras,
Chennai-600036, India
Adg@ee.iitm.ac.in

Nandita Dasgupta
Indian Institute of Technology Madras,
Chennai-600036, India
Nand@ee.iitm.ac.in

Maggy Colas
recherches CNRS-HDR
IRCER-UMR CNRS 7315
12 rue Atlantis
maggy.colas@unilim.fr

Raphael Sommet
Xlim laboratory
7 rue Jules Vallès
19100 Brive-La-Gaillarde, FRANCE
raphael.sommet@xlim.fr

Abstract— This paper investigates the influence of carbon doping GaN buffer and the addition of a GaN cap layer on the thermal properties of gallium nitride high electron mobility transistors (GaN HEMTs). These devices are renowned for their excellent electrical characteristics, such as high operating frequency and high breakdown voltage. Recent developments, including carbon doping of the GaN buffer and integration of a GaN cap layer, aim to improve the crystalline quality, the charge carrier mobility and reduce the conduction losses. Thermal analysis using the thermoreflectance technique was carried out to assess the impact of these modifications on the thermal resistance of the transistors. Four different samples were fabricated and studied, with various combinations of doping and capping layers.

Keywords—GaN HEMT's, Thermoreflectance, Thermal measurement, GaN C-doping, GaN Cap layer, Thermal resistance.

I. INTRODUCTION

The high electron mobility transistor based on gallium nitride (GaN HEMT) has attracted the attention of researchers because of its remarkable characteristics, in particular its high operating frequency and high breakdown voltage[1]. In addition, these devices are also capable of generating high current densities and maintaining low channel resistances thanks to their high electron mobility and high carrier concentration. In recent years, this technology has continued to evolve, making these devices even more powerful and reliable. These developments include the integration of the GaN cap layer and the carbon doping of the GaN buffer to reduce current collapses, attenuate surface defects, and increase the crystalline quality of the material, resulting in electrical improvements such as increased charge carrier mobility and reduced conduction losses.

Although these developments have significantly improved the electrical properties of these components, their impact on the thermal properties of the devices still needs to be assessed. Thus, in this paper, a thermal analysis based on the

thermoreflectance imaging technique is carried out to determine how the introduction of the GaN cap Layer and the doping of the GaN buffer influence the thermal resistance of a 2x50 μ m GaN HEMT.

II. DIVICES FABRICATION

The wafers used in this study were grown by Veeco Instruments Inc., USA, in a Propell Metal Organic Chemical Vapor Deposition (MOCVD) reactor on 6-inch-high resistive silicon (HR-Si) substrates. Figure 1 shows the schematic cross-section of the wafers. GaN HEMTs were fabricated on four different GaN-on-Si wafers. Let us denote the wafers as “wafer A,” “wafer B,” “wafer C,” and “wafer D.” 10 nm of In_{0.17}Al_{0.83}N is used as a barrier layer in all wafers. For the Al mole fraction of 0.83, the lattice constant of InAlN matches with the GaN buffer layer. As a result, In_{0.17}Al_{0.83}N forms a strain-free barrier layer, which prevents the inverse piezoelectric effect at high voltage operations and improves the breakdown voltage of HEMTs. Between the In_{0.17}Al_{0.83}N barrier and GaN buffer layer, 1 nm of AlN spacer layer is used in all wafers. AlN spacer layer reduces carrier scattering and improves the mobility of electrons. Though Wafer A and wafer C do not have a GaN cap layer, wafer B and wafer D contain 2 nm of GaN cap layers. GaN cap layer reduces surface traps, off-state gate, and drain leakage current and increases 2-DEG electrons mobility, breakdown voltage, and f_T of HEMTs [2]. The GaN buffer layers of wafer A and wafer B are unintentionally doped. UID:GaN is usually n-type due to nitrogen vacancies[3] and/or background oxygen doping[4]. GaN HEMTs with n-type UID:GaN usually have higher leakage current and lower breakdown voltage. Sometimes, the GaN buffer layer is counter-doped with carbon to improve leakage current and breakdown voltage. C-doped GaN buffer layer improves breakdown voltage, reduces leakage current, and helps in realizing near-ideal subthreshold swing[5]. The buffer layer of wafers C and D is divided into three sub-layers. A C-doped layer with a doping concentration of 2x10¹⁹ per cm³ is sandwiched between two UID: GaN in the buffer layers of wafer C and wafer D. Below the GaN

buffer layers, AlGaIn strain relief layers and AlN nucleation layers are used in all wafers. The AlGaIn strain relief layers are divided into three sub-layers with Al mole fractions of 75%, 50%, and 25% from the AlN interface to UID: GaN interface. The total thickness of the GaN buffer layer, AlGaIn strain relief layer and AlN nucleation layer is 1.7 μm .

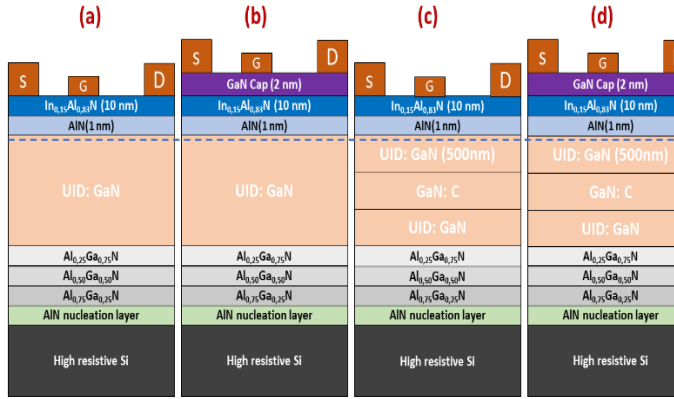


Figure 1 : Schematic layer structure of the wafer; (a) without GaN cap and no carbon doping, (b) with GaN cap but no carbon doping, (c) without GaN cap but with carbon doping, (d) with GaN cap and carbon doping in the GaN buffer layer.

The fabrication process started by cleaning the wafers by boiling in trichloroethylene and acetone for five minutes each, followed by lithography to open windows for source and drain contacts. Next, the samples were dipped in dilute HCl (DI water: HCl = 10:1) for 1 min to remove any native oxide and immediately loaded in an electron beam evaporation system to deposit Ti/Al/Ni/Au (30/140/40/100 nm) metal stack. After source-drain patterning by lift-off, the samples were annealed in N_2 ambient at 810 $^\circ\text{C}$ for 60 seconds for the ohmic contact formation. Mesa isolation etching was then performed in Inductively Coupled Plasma Reactive Ion Etching (ICP-RIE) using Cl_2/BCl_3 plasma to a depth of 200 nm. Next, gate lithography was carried out in an e-beam lithography system using PMMA-A8 as an e-beam resist, and the samples were again dipped in dilute HCl (DI Water: HCl = 10:1) for 1 min prior to gate metal (Ni/Au 30/80 nm) deposition. The gate metal was patterned by the standard lift-off process. Contact pad metal Ni/Au (40/80 nm) was deposited by e-beam evaporation. Finally, the samples were annealed at 400 $^\circ\text{C}$ in N_2 ambient for 5 minutes. The source-to-drain separation of the devices is 6 μm , and the gate length is 300 nm, placed at the middle of the source and drain.

III. THERMOREFLECTANCE METHOD FOR TEMPERATURE MEASUREMENTS

Thermoreflectance is a temperature measurement technique that leverages the optical changes in a material resulting from temperature variations. This method is based on the principle that the optical properties of materials, such as refractive index and reflectance, are temperature-dependent [6]. These optical changes affect the way the material reflects light. By directing a beam of light onto the surface of the material and measuring changes in the reflected light, it is possible to determine temperature variations at the material surface with a high degree of accuracy. This method is particularly useful for applications where temperature measurements with high spatial resolution is required. This technique is non-destructive and allows for the acquisition of detailed temperature maps thanks to the CCD camera, which

captures high-resolution spatial variations in temperature. By analysing the changes in reflectance at each pixel, researchers can create precise thermal mapping of the material's surface.

During measurement, the materials constituting the transistor undergo thermal expansion due to changes in temperature. This technique requires the integration of several peripheral systems to ensure an accurate and successful measurements. Notably, a piezoelectric system is essential.

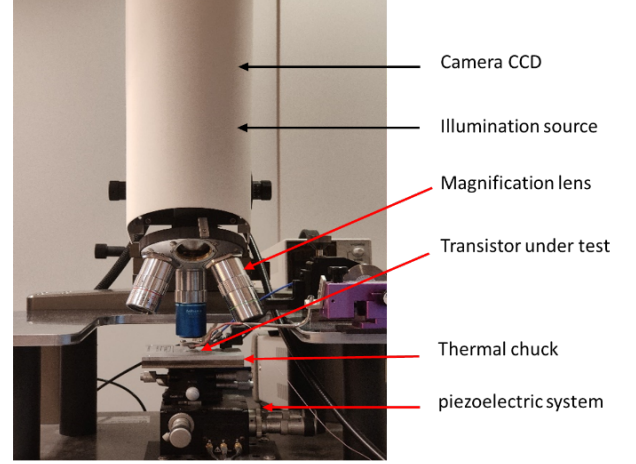


Figure 2 :Illustration of the Microsanj measurement bench based on thermoreflectance

Figure 2 illustrates the Microsanj measurement bench based on thermoreflectance available at Xlim. It is composed of a light source capable of generating four optical sources offering different wavelengths, 365nm, 470 nm, 530 and 680 nm, and four objectives (x10, x25, x50 and x100) suitable for these wavelengths, a piezoelectric position correction system to compensate for movements caused by the expansion of materials when heated, a CCD camera for analysing the reflected optical signal and an electrical excitation source for applying the dissipated power to the devices. The thermoreflectance technique uses a beam of monochromatic light that is directed at the surface of the material, the reflected light is then analysed to detect variations induced by changes in temperature. Variations in reflectance and other optical properties are then converted into temperature measurements. The dependence of the relative variation of surface reflectance on surface temperature can be expressed by the following equation [6], [7].

$$\frac{\Delta R}{R_0} = C_{th}(x, y, \lambda) \cdot \Delta T \quad (1)$$

Where C_{th} is the thermoreflectance coefficient which depends on material properties and on the illumination source wavelength. The measurements were carried out on the four different structures to highlight the thermal impact of the integration of the GaN cap layer and the carbon doping of the GaN buffer. To perform this measurement, two steps are required. The first one is the calibration step, during which a known temperature difference is applied to the transistor using a thermal stage, typically $\Delta T = 50^\circ\text{C}$. This induced temperature difference leads to a change in reflectivity, which is measured as a variation in reflectance. Another important parameter to consider is the wavelength of the incident light, as the thermoreflectance coefficient is highly sensitive to it. Therefore, it is crucial to select the wavelength that maximizes the thermoreflectance coefficient for accurate and effective measurements.

Previous studies on GaN transistors have demonstrated that the area that undergoes the most significant heating is the part of the channel located under the gate on the drain side. This is due to the high electric field present in this region, which can be over 100 times greater than in other channel regions [8], [9]. The measurement zone targeted in this work is the region between the gate and the drain as shown in **Erreur ! Source du renvoi introuvable**. The measurement was therefore carried out on the GaN material which is one hundred nanometres above the hotspot. During the calibration stage, several wavelengths were used to determine the optimum wavelength. Figure 3 shows the dependence of the thermoreflectance coefficient for 4 different wavelengths. The wavelength chosen was 365nm, which gives the highest thermoreflectance coefficient in absolute terms with $C_{th} -3,18 \times 10^{-3} K^{-1}$ on the GaN material.

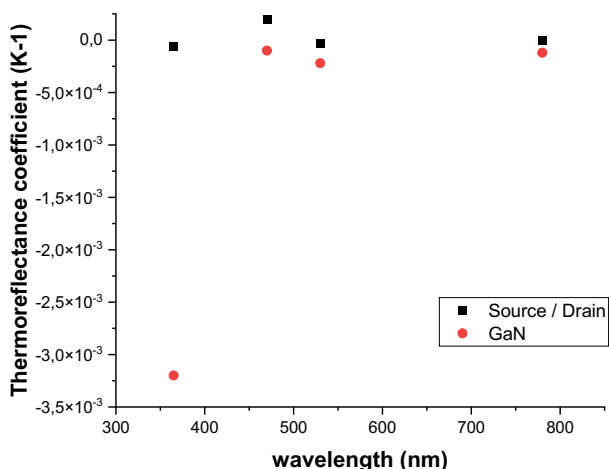


Figure 3 : Thermoreflectance Coefficient as a Function of Wavelength of source, drain and GaN materials.

Once extracted, this thermoreflectance coefficient is used in the second step, which consists of applying a dissipated power to the transistor and measuring the corresponding change in temperature, and this for several dissipated powers.

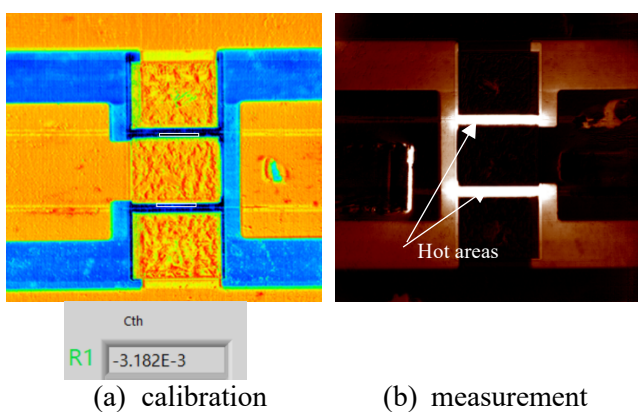


Figure 4 : CCD image, (a) calibration step where R1 is C_{th} of the GaN material between gate and drain and (b) measurement step.

The thermal resistance is then calculated according to Equation 2 to compare the results of the four transistors. This allows us to assess the thermal impact of the integration of the GaN cap layer and the carbon doping of the GaN buffer. By evaluating these factors, we can better understand how they influence the transistors thermal performance. Thermal

resistance measures the component's ability to conduct heat, and is expressed as the ratio between the rise in temperature within the transistor and the corresponding dissipated power.

$$R_{th} = \frac{\Delta T}{P_{diss}} \quad (2)$$

Where ΔT is the temperature rise in $^{\circ}C$ and P_{diss} is the applied dissipated power in W . A lower thermal resistance indicates a better ability to dissipate heat. As a result, a sample with low thermal resistance is more efficient in terms of temperature management, contributing to more stable performance and longer lifespan.

IV. RESULTS AND DISCUSSIONS

Measurements were carried out for various dissipated powers, and the corresponding thermal resistance values for the four transistors are shown in .

The results show that sample C has the highest thermal resistance, as it has no GaN capping layer and its buffer layer is carbon-doped. On the other hand, the thermal resistance is lowest for sample B, which has a GaN cap layer and its buffer layer is not doped with carbon.

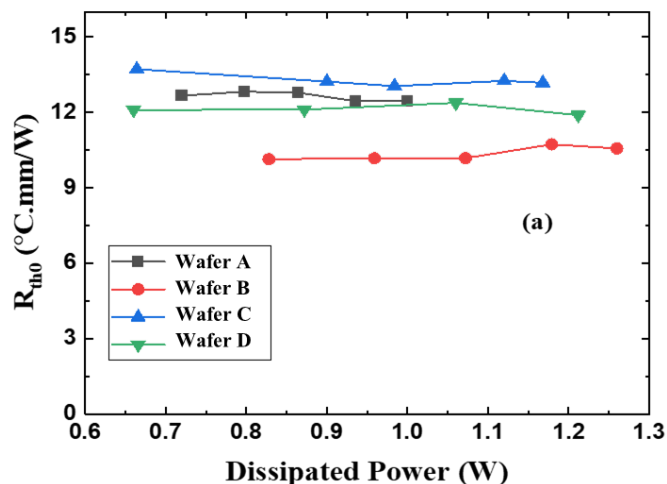


Figure 5 :Thermal resistance as a function of the power dissipated for the four configurations of the GaN transistor, $2 \times 50 \mu m$

The clearest observation from the experimental results is the significant influence of the high carbon doping on the thermal resistance of GaN-based transistors, a phenomenon observed independently of the presence or absence of a GaN cap layer. In fact, sample C, with no cap layer and doped with carbon, has the highest thermal resistance. This is due to the defects induced by the carbon atoms in the crystalline structure, which interfere with the thermal conduction, thereby reducing the efficiency of heat dissipation. Similarly, even in the presence of a capping layer, carbon doping also plays a part by increasing thermal resistance. These results are consistent with other work done by J. Zou and All [10] which shows that doping has a negative impact on the thermal conductivity of semiconductors.

The results for the GaN cap layer should be interpreted with caution. Thermoreflectance measurement is a "surface technique", which means that it assesses the temperature at the surface of the sample. Therefore, in samples with a cap layer, the measurement is performed at the surface of this layer, i.e. approximately 2 nm higher than for samples without GaN cap. However, this thickness is still very small (2nm), allowing this

measurement and comparison to remain relevant for assessing the differences in thermal performance between the samples.

V. CONCLUSION

The results show that carbon doping of the GaN buffer significantly increases the thermal resistance of the transistors, independently of the presence of a GaN cap layer. The sample without a GaN Cap layer but doped with carbon showed the highest thermal resistance, attributed to the structural defects introduced by the carbon atoms, which disrupt thermal conduction. In contrast, the sample with a GaN cap layer and no carbon doping showed the lowest thermal resistance, illustrating the beneficial effect of the cap layer on heat dissipation. Although thermoreflectance measurement is a surface technique, the results are still relevant for assessing differences in thermal performance between samples. These findings highlight the importance of precise control of doping and layer structure to optimise the thermal and electrical performance of GaN HEMT devices.

ACKNOWLEDGMENT

The authors would like to acknowledge the financial support from Labex/Sigma-Lim and TAS company.

This work is supported by the CNRS International Research Project (IRP) “MEGATRON - Project MEMS and GaN Development ThRough COmplementary CollaboratioN”.

This research work benefited from the support of the Platinom platform, with funding from Nouvelle Aquitaine council and the European Union under the PILIM program.

The authors would like to acknowledge the Centre for NEMS and Nanophotonics (CNNP), Indian Institute of Technology Madras, for providing the fabrication and characterization facility. The authors would like to acknowledge Veeco Instrument Inc. USA, for providing the wafers

REFERENCES

- [1] U. K. Mishra, P. Parikh, and Yi-Feng Wu, ‘AlGaIn/GaN HEMTs—an overview of device operation and applications’, *Proc. IEEE*, vol. 90, no. 6, pp. 1022–1031, Jun. 2002, doi: 10.1109/JPROC.2002.1021567.
- [2] S. Sarkar, R. P. Khade, A. DasGupta, and N. DasGupta, ‘Effect of GaN cap layer on the performance of AlInN/GaN-based HEMTs’, *Microelectron. Eng.*, vol. 258, p. 111756, Apr. 2022, doi: 10.1016/j.mee.2022.111756.
- [3] Shih-Chien Liu, Bo-Yuan Chen, Yueh-Chin Lin, Ting-En Hsieh, Huan-Chung Wang, and E. Y. Chang, ‘GaN MIS-HEMTs With Nitrogen Passivation for Power Device Applications’, *IEEE Electron Device Lett.*, vol. 35, no. 10, pp. 1001–1003, Oct. 2014, doi: 10.1109/LED.2014.2345130.
- [4] B.-C. Chung and M. Gershenson, ‘The influence of oxygen on the electrical and optical properties of GaN crystals grown by metalorganic vapor phase epitaxy’, *J. Appl. Phys.*, vol. 72, no. 2, pp. 651–659, Jul. 1992, doi: 10.1063/1.351848.
- [5] S. Sarkar, R. P. Khade, A. Shanbhag, N. DasGupta, and A. DasGupta, ‘Near-Ideal Subthreshold Swing in InAlN/GaN Schottky Gate High Electron Mobility Transistor Using Carbon-Doped GaN Buffer’, *IEEE Trans. Electron Devices*, vol. 69, no. 8, pp. 4408–4413, Aug. 2022, doi: 10.1109/TED.2022.3181539.
- [6] D. Pierścińska, ‘Thermoreflectance spectroscopy—Analysis of thermal processes in semiconductor lasers’, *J. Phys. Appl. Phys.*, vol. 51, no. 1, p. 013001, Jan. 2018, doi: 10.1088/1361-6463/aa9812.
- [7] M. Farzaneh *et al.*, ‘CCD-based thermoreflectance microscopy: principles and applications’, *J. Phys. Appl. Phys.*, vol. 42, no. 14, p. 143001, Jul. 2009, doi: 10.1088/0022-3727/42/14/143001.
- [8] M. Hosch, J. Pomeroy, A. Sarua, M. Kuball, H. Jung, et H. Schumacher, ‘Field dependent self-heating effects in high-power AlGaIn/GaN HEMTs’, May 2009.
- [9] M. Kuball and J. W. Pomeroy, ‘A Review of Raman Thermography for Electronic and Opto-Electronic Device Measurement With Submicron Spatial and Nanosecond Temporal Resolution’, *IEEE Trans. Device Mater. Reliab.*, vol. 16, no. 4, pp. 667–684, Dec. 2016, doi: 10.1109/TDMR.2016.2617458.
- [10] J. Zou, D. Kotchetkov, A. A. Balandin, D. I. Florescu, and F. H. Pollak, ‘Thermal conductivity of GaN films: Effects of impurities and dislocations’, *J. Appl. Phys.*, vol. 92, no. 5, pp. 2534–2539, Sep. 2002, doi: 10.1063/1.1497704.